Methods for sampling sequential annual bone growth layers for stable isotope analysis

Calandra N. Turner Tomaszewicz[1,2]*, Jeffrey A. Seminoff[2], Larisa Avens[3] and Carolyn M. Kurle[1]

[1]*Division of Biological Sciences, Ecology, Behavior and Evolution Section, University of California, San Diego, La Jolla, CA 92093-0116, USA;* [2]*Southwest Fisheries Science Center, NOAA, National Marine Fisheries Service, La Jolla, CA 92037, USA; and* [3]*Southeast Fisheries Science Center, NOAA, National Marine Fisheries Service, Beaufort, NC 28516, USA*

Summary

1. Stable carbon (δ^{13}C) and nitrogen (δ^{15}N) isotope analysis (SIA) has proven useful in addressing fundamental questions in ecology such as reconstructing trophic interactions, habitat connections and climate regime shifts. The temporal scales over which SIA can be used to address ecological problems vary depending on the protein turnover times of the analysed tissue. Hard, inert tissues, such as teeth, bones and mollusc shells, grow in regular intervals (i.e. daily or annually), and sequential sampling of these growth layers provides a time series of isotopic patterns. As a result, SIA on these tissues is useful for elucidating behaviour and ecology of animals over time, especially those with cryptic life-history stages, such as marine turtles that retain growth layers in their humerus bones. To date, there exists no standard protocol for the sequential sampling of cortical bone samples taken from fresh, modern samples for SIA.

2. We tested two different methods, micromilling untreated bone cross sections and biopsy coring bone cross sections processed for skeletochronology, for sequentially sampling individual growth layers from marine turtle humerus bones.

3. We present a standard protocol for sequential bone growth layer sampling for SIA, facilitating direct comparison of future studies. We recommend using the micromilling sampling technique on untreated bone cross sections, as it facilitated higher precision sampling of growth layers that were not affected by chemical processing, and minimized sample handling, thereby reducing chances for contamination.

4. This is the first study to present a standardized method to sequentially sample annual bone growth layers for stable isotope analysis and facilitates direct comparison among future studies.

Key-words: bone, collagen, marine turtles, sequential sampling, skeletochronology, stable isotope analysis

Introduction

Stable carbon (δ^{13}C) and nitrogen (δ^{15}N) isotope analysis (SIA) of organic matter is a powerful tool used in ecological studies to elucidate diet, trophic level, habitat use and migration of a wide variety of taxa in both marine (e.g.Vander Zanden & Rasmussen 2001; Michener & Lajtha 2007; Graham *et al.* 2010; Newsome, Clementz & Koch 2010) and terrestrial (e.g. Koch, Fogel & Tuross 1994; Hobson, Barnett-Johnson & Cerling 2010) systems. Examination of both δ^{13}C and δ^{15}N values from animal tissues allows for reconstruction of animal movement patterns due to spatial variation in these values that reflect differential carbon and nitrogen processing at the base of terrestrial and marine food webs (DeNiro & Epstein 1978; Rau *et al.* 1983; Clementz & Koch 2001; McMahon, Hamady & Thorrold 2013).

Different tissues incorporate and retain stable isotopes from the diet at varying rates, allowing researchers to investigate foraging ecology over multiple time-scales by sampling-specific

tissues (Hobson 1999; Dalerum & Angerbjörn 2005; Reich, Bjorndal & Martinez del Rio 2008; Kurle 2009). Many hard tissues, such as bone, teeth, otoliths, corals and bivalve shells, do not have regular cellular turnover; instead, subsequent layers formed during growth are retained. These inert layers preserve their original chemical composition, thereby reflecting the stable isotope values of the environment and the prey consumed during the formation of a particular growth layer (e.g. Elorriaga-Verplancken *et al.* 2013). This creates a time series of data reflecting an animal's diet and location when layers are formed at regular time intervals (e.g. days for otolith rings, or years for bone, tooth, coral and tree rings).

Sequential SIA of growth layers has been conducted on tissues such as otolith and teeth (e.g. Schwarcz *et al.* 1998; Hobson 1999; Newsome *et al.* 2006; Elorriaga-Verplancken *et al.* 2013) with promising results for reconstructing habitat use patterns for migratory megafauna. For some marine turtle species, humerus bone tissue is deposited in annual layers (e.g. Snover *et al.* 2011) and, recently, sequential SIA of marine turtle bone growth layers identified by skeletochronology has been successful, generating a time series reflecting the diet and

*Correspondence author. E-mail: cturnert@ucsd.edu

habitat of an individual turtle over multiple years (Snover *et al.* 2010; Avens *et al.* 2013). However, no standard sequential sampling methods have yet been described for SIA of $\delta^{13}C$ and $\delta^{15}N$ values from annual bone layers. Standardizing a protocol that combines these two methods, SIA with skeletochronology, could provide a reproducible approach to address important questions on the ecology and life history of many vertebrate species that do not possess teeth or otoliths, and could be especially useful for the study of migratory endangered animals such as marine turtles.

Here, we present and compare two methods to be used in combination with skeletochronology to sequentially sample individual bone growth layers for SIA. The establishment of a standard protocol will allow for future bone SIA studies to proceed with greater efficiency and accuracy, eliminate the potential for inconsistencies among methods examining ecological questions using bone SIA, and allow for more direct comparisons among studies. Our techniques were developed specifically for marine turtles, but can be applied to other species where annual growth in bone layers has been validated.

Methods

MARINE TURTLE BONE SAMPLES

We developed two methods, micromilling untreated bone cross sections and biopsy coring skeletochronology-processed bone cross sections, to sample sequential growth layers for SIA from marine turtle humerus bones obtained following sea turtle skeletochronology

processes (Goshe *et al.* 2009; Avens *et al.* 2012). We also conducted experimental trials to test for the effects of inorganic carbon removed via acidification, and lipid extraction, on the accurate measure of the $\delta^{13}C$ and $\delta^{15}N$ values from bone material, and those data are presented elsewhere (Turner Tomaszewicz *et al.* 2015). Of relevance here, Turner Tomaszewicz *et al.* (2015) found that lipid content of cortical bone from modern turtles was low, based on the carbon:nitrogen ratio (C:N) of <3·5, thus negating the need for lipid extraction as recommended by Post *et al.* (2007). As part of a larger study, we collected the humerus bones from dead-stranded east Pacific green sea turtles (*Chelonia mydas*) (*n* = 5) and North Pacific loggerhead sea turtles (*Caretta caretta*) (*n* = 5). All samples collected were from juvenile and subadult turtles of similar size at stranding (between 53 and 73 cm curved carapace length, CCL), and all turtles stranded between 2004 and 2011 at a single beach (Playa San Lázaro) adjacent to a high-turtle density foraging area along the Pacific coast of Baja California Sur, Mexico (Seminoff *et al.* 2014).

SEQUENTIAL SAMPLING OF BONE GROWTH LAYERS

Technique one: Micromilling

Bones were prepared according to marine turtle skeletochronology processes as described in Goshe *et al.* 2009, 2010; and Avens *et al.* 2012; but modified for SIA sampling. Two 3-mm sections were cut from the whole bone using an Isomet slow-speed saw (Buehler) fitted with a diamond wafering blade (Buehler) (Fig. 1a). Next, the Isomet saw blade was used to make two 0·5-mm-deep notches in the dorsal side of both 3-mm sections, and these notches were used to align the two cross sections in later sequential sampling steps (Fig. 2b). After the notches were made, one cross section was chemically processed for skeletochronology and will be referred to as the 'skeletochronology-
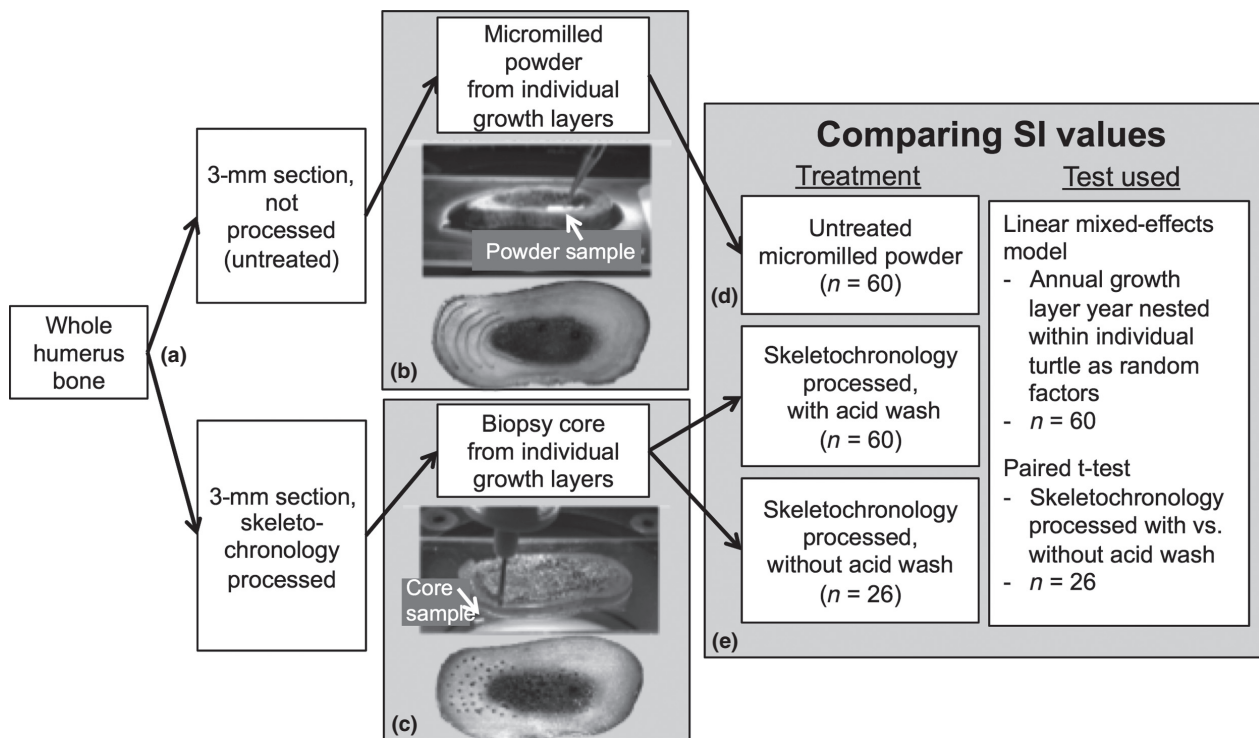

Fig. 1. Experimental flow chart. (a) two cross sections cut from humerus bone; (b) individual bone growth layers sampled by micromill; (c) individual bone growth layers sampled by biopsy core; (d) paired micromilled groups; (e) matched biopsy cored groups.
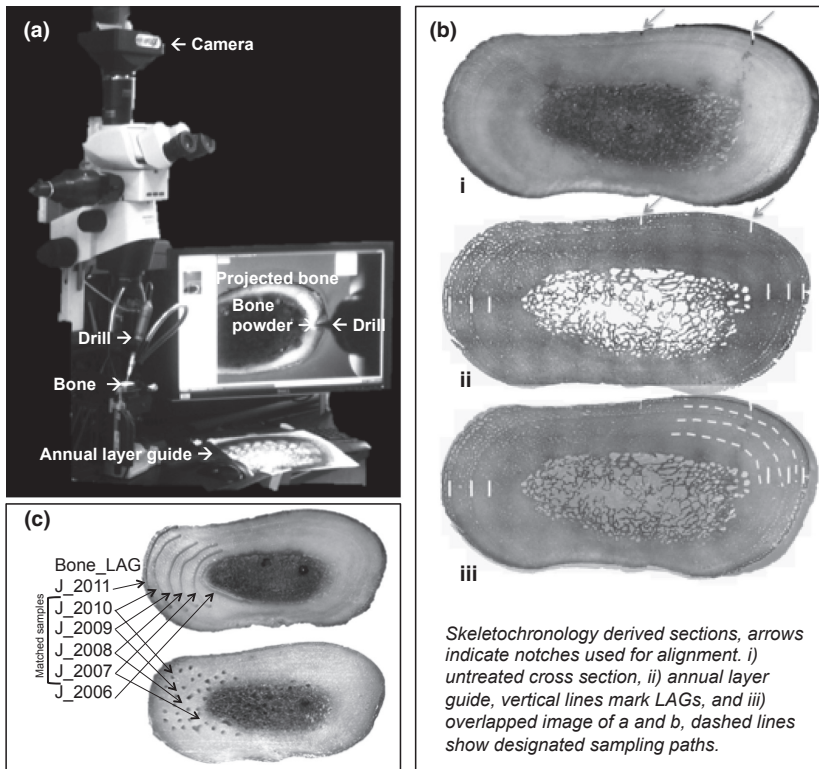
Fig. 2. Sampling set-up and design. (a) Micromill sampling showing camera, drill, bone, projected bone image, drilled bone powder and annual layer guide. (b) Matched annual samples from a single bone, top: groves show where micromilled samples extracted; bottom: holes show where biopsy cored samples extracted. (c) Bone to be sampled (i) untreated bone with notches, (ii) untreated bone is then aligned with annual layer guide, (iii) to generate sampling drill plan.

Skeletochronology derived sections, arrows indicate notches used for alignment. i) untreated cross section, ii) annual layer guide, vertical lines mark LAGs, and iii) overlapped image of a and b, dashed lines show designated sampling paths.

processed' cross section, whereas the second, paired cross section was not processed for skeletochronology, and hereafter referred to as the 'untreated' cross section (Fig. 1).

We identified individual growth layers in the bone sections with a skeletochronology-derived image that we call the 'annual layer guide'. This guide is an image of the bone cross section showing each annual growth layer, which is separated by a distinct line of arrested growth (LAG). We labelled each LAG identified during the skeletochronology processing, and digitized the image (Snover & Hohn 2004; Goshe *et al.* 2009; Snover *et al.* 2011). After printing the annual layer guide image onto standard transparency film, the image was taped directly on a computer monitor. We then positioned the untreated bone section beneath an Olympus SZX10 microscope, fitted with an Olympus Spot-Flex camera (U-CMAD-2; Fig. 2a), and the image of the bone section was displayed on the computer monitor fitted with the annual layer guide transparency, and both images were aligned (Fig. 2a).

We used a computer-guided micromilling system (Carpenter Microsystems CM-2, version 3.0.6, Iowa City, IA, USA) for individual growth layer sampling. We programmed sampling paths using the CM-2 micromilling system and extracted ~1·5 mg of bone powder from individual growth layers of the untreated cross section, one growth layer at a time, using an NSK Volvere Vmax drill at 10 000 rpm, fitted with a 0·10-mm carbide, round-tipped bit (model H71.11.004 by Brasseler USA Dental Instruments; Fig. 1b).

Prior to drilling and extracting samples from each untreated bone cross section, we outlined a sampling plan based on annual layer width, sample location and the proximity to the bone centre. Specifically, we sampled inner layers preferentially before exterior samples to avoid sample loss during drilled-powder collection, and ensure single-growth layer sampling. Further, we only sampled growth layers contained in the compact cortical bone, avoiding all areas of the central resorbed and vascularized bone. The central, vascularized region was avoided because (i) the growth layers have been, or are in the process of being, resorbed and (ii) the cellular turnover and molecular exchange differs in

comparison with the cortical bone and would not yield isotope values that are comparable to cortical bone. We were able to sample thin growth layers (0·25–0·10 mm) by first drilling away and discarding adjacent layers, which then isolated the target layer. Between sampling sequential growth layers, we removed any excess bone powder, dust or other debris from the surface of the bone cross section using compressed air.

Untreated cross sections were affixed to 25 × 75 mm glass slides using 3–5 drops of glue (Advanced Performance Instant Adhesive RP 100, by Adhesive Systems Inc., Frankfort, IL, USA), and allowed to dry for at least 24 h prior to sampling. The 1·5 mg of bone dust from the sampling path of each growth layer was obtained by drilling to a depth of ~400 μm (10-μm increments over ~40 passes; Fig. 1b). To minimize the chance of sampling non-target growth layers, we avoided drilling deeper than ~400 μm because the location of LAGs often shifts slightly through the length of the bone, a common characteristic of growth layers. Upon completion of drilling each annual growth layer, we tapped the drilled bone powder onto a sheet of weigh paper, and weighed 1·5 mg of bone powder into tin capsules for SIA.

Technique two: Biopsy coring

Upon completion of skeletochronology chemical processing, a soft, flexible cross section is archived. We assessed the utility of sampling growth layers from these previously archived cross sections for SIA. We tested for this because, if these samples prove to successfully yield accurate $\delta^{13}C$ and $\delta^{15}N$ values, then a significant number of archived bone samples would become available for future SIA studies on marine turtle populations world-wide. The skeletochronology chemical processing leaves the cross sections pliable, precluding growth layer sampling with the micromilling technique and necessitating a different sequential sampling method we developed. Chemical processing steps and storage of these cross sections during skeletochronology include

fixation for ~2 h in 10% formalin, followed by a water rinse, then decalcification in a commercial agent that varies depending upon turtle bone type (Snover & Hohn 2004; Goshe *et al.* 2009, 2010). This decalcification step is analogous to the decalcification via acidification that was tested on cortical bone powder samples elsewhere (Turner Tomaszewicz *et al.* 2015).

The skeletochronology-processed bone cross sections were soaked for 6–37 h in RDO, a commercial decalcifying agent consisting of HCl (Apex Engineering, Aurora, IL, USA). Upon completion of the skeletochronology processing, the cross sections were archived in 100% glycerine. All samples used in this study had been archived and stored in glycerine for 1–2 years. Prior to use for sequential sampling in this study, glycerine-archived samples were transferred to a 1:1 glycerine: water solution for 1 day before transfer to soak in ultra-pure (MilliQ, Darmstadt, Germany) water for 3 days. The water was changed daily.

Skeletochronology-processed cross sections were placed on, but not affixed to, 25 × 75 mm glass slides, and positioned under the same microscope and camera set-up used for the micromilling method. These samples naturally adhered to the glass slides and were adjusted manually to align with the annual layer guide transparency affixed to the computer monitor described above. Each skeletochronology-processed cross section ranged from 1 to 3 mm in thickness, and we extracted samples from each growth layer using 0·5-mm-diameter biopsy punches (Harris Uni-core FTIR cardpunches, Ted Pella, Redding, CA, USA). This method is modified from one used to sample dentine growth rings for archaeological studies (Burt & Garvie-Lok 2013). The biopsy punches removed small cores from the decalcified bone that were ejected into a cryovial for further processing (Fig. 1c). In order to obtain enough material for SIA, we removed a total of 4–10 cores from each individual annual growth layer and, to accommodate the diameter of the biopsy punch, we targeted annual layers that were at least 0·5 mm in width. In some cases, a scalpel was used to collect samples from annual layers located near the outer edge of the cross section that were too thin for proper removal with the biopsy punch. All biopsy core samples were oven dried at ~50°C for 24–48 h before preparation for SIA.

To ensure that complete demineralization occurred during the skeletochronology processing, a subset of growth layers ($n = 26$) were sampled twice, and one sample of each pair was washed in with a weak acid (0·25 M HCl), following the method described by Turner Tomaszewicz *et al.* (2015; see Supporting information for additional details). Paired *t*-tests were used to examine the δ^{13}C and δ^{15}N values with and without the HCl acid wash.

STABLE ISOTOPE ANALYSIS

We analysed all samples for δ^{13}C, δ^{15}N, per cent carbon (%C), and per cent nitrogen (%N). Samples were analysed by combustion in a Carlo Erba NA 1500 CNS elemental analyser interfaced via a ConFlow II device to a Thermo Electron DeltaV Advantage isotope ratio mass spectrometer in the Stable Isotope Geochemistry Laboratory at the University of Florida, Gainesville. A conventional delta (δ) notation in parts per thousand or permil (‰) was used to express the stable isotope ratios of the samples relative to the isotope standards:

$$\delta X = ([R_{sample}/R_{standard}] - 1),$$

where the corresponding ratios of heavy to light isotopes (^{13}C/^{12}C and ^{15}N/^{14}N) in the sample and standard are represented by R_{sample} and $R_{standard}$, respectively. $R_{standard}$ for δ^{13}C was Vienna Pee Dee Belemnite and $R_{standard}$ for δ^{15}N was atmospheric N$_2$. Laboratory reference materials, USGS40 (L-glutamic acid), were calibrated at regular intervals against the standards. Precision for these data was determined using the standard deviations around the means for a subset of the internal laboratory standards run at set intervals. Standard deviations for samples ranged from 0·03 to 0·20‰ for δ^{13}C and from 0·02 to 0·24‰ for δ^{15}N, with mean (±SD) precisions of 0·08 ± 0·05‰ and 0·13 ± 0·08‰, respectively.

The C:N ratios for all samples were calculated by dividing %C by %N, and we used the %C and %N values to assess protein purity and material composition for the micromilled bone powder based on typical bone composition percentages. The %C and %N of whole bone is generally ~15% and ~5%, respectively, whereas the %C and %N of collagen is generally ~45% and ~15%, respectively. Pure, unaltered protein, including collagen, has a C:N ratio between 2·9 and 3·6 (Schoeninger *et al.* 1989; Ambrose 1990; Koch, Fogel & Tuross 1994; Van Klinken 1999).

STATISTICAL ANALYSIS

Absolute difference in δ^{13}C and the δ^{15}N values was compared between the untreated micromilled samples and the skeletochronology-processed biopsy core samples and was calculated as δ^{13}C$_{skeletochronology-processed}$ − δ^{13}C$_{untreated}$, and similar for effect on δ^{15}N. We evaluated the effect of skeletochronology processing on the δ^{13}C and δ^{15}N values of the biopsy cores using a linear mixed-effects model. Because this trial included multiple samples from different years from individual turtles, we assigned 'year' nested within 'individual turtle' as random factors to examine variation attributed to skeletochronology treatment and turtle species:

$$lme(\delta^{13}C(\text{ or }\delta^{15}N) \sim \text{Species*Treatment, random} = \sim 1|\text{Turtle/Year}).$$

Samples with low lipid content (C:N < 3·5 for aquatic consumers) generally do not require lipid extraction for SIA (Post *et al.* 2007). We eliminated any samples with C:N ratios >3·5. We used the software program R for all analyses (R Core Development Team 2013), package 'NLME' for the linear mixed-effects model, and significance was tested at the level of $\alpha = 0·05$.

Results

SEQUENTIAL SAMPLING

The two sequential sampling methods tested, micromilling and biopsy coring, were effective for physically extracting annual bone growth layer samples. Samples from multiple growth layers were removed from each of the ten turtle bones. There was no significant effect of the HCl wash on either δ^{13}C values ($t_{25} = -1·23$, $P = 0·23$) or δ^{15}N values ($t_{25} = 0·03$, $P = 0·97$) of the skeletochronology-processed biopsy cores; therefore, the rest of the analysis was conducted on the 60 biopsy core samples that had been acidified. We extracted samples from a total of 60 different annual growth layers from each the untreated cross sections, and the skeletochronology-processed cross sections and directly compared these paired samples (Table 1, Fig. 2c). The amount of time required to extract a single annual growth layer sample by micromilling was ~1–2 h, whereas a single sample (4–10 cores) removed by biopsy coring took ~15 min.

The micromilling method more precisely sampled individual growth layers, in comparison with the biopsy coring method, because the drill used to sample the untreated cross sections

Table 1. Experiment set-up and design

| Origin | Species | Turtle sample size | Sample size unique turtle and year | | |
			Micromilled Untreated	Skeletochronology-Processed w/HCl	Skeletochronology-Processed w/o HCl
Pacific	Cm	5	27	27	13
	Cc	5	33	33	13
Total sample size		10	60	60	26

Number of samples used for the biopsy cores, all samples were from individual growth layers. The sample size for each group shown is the total number of samples from a unique turtle and year, for each species, that were compared as paired samples.

remained in a fixed position and was constantly aligned with the annual image guide during sample extraction. In contrast, there was some unintentional and unavoidable movement of the hand-held biopsy punch during sampling of the skeletochronology-processed cross sections, resulting in possible misalignment with the annual image guide, and therefore lower confidence that every sample was removed from the intended growth layer. Further, the samples extracted using the micromilling method had a lower chance of contamination as they were only handled once, when the drilled bone powder was tapped on to a weigh sheet and then directly placed into a tin capsule for SIA. The biopsy core samples, contrastingly, were handled multiple times, potentially increasing the likelihood of a sample being contaminated. Repeated handling occurred (i) as each sample was initially collected, then oven dried, then weighed, and (iii) because multiple cores (4–10) were collected from each individual growth layer to collect enough mass for SIA.

WHOLE BONE POWDER VS. BONE CORES PROCESSED FOR SKELETOCHRONOLOGY

Based on the C:N ratios, %C and %N values, micromilled powder samples from the untreated cross sections reflected whole bone composition (%C 14·29 ± 2·48 and %N 4·41 ± 0·72), whereas the skeletochronology-processed biopsy core samples reflected characteristic collagen values (C% 42·87 ± 1·04 and %N 14·87 ± 0·38; Fig. S1, Table S1). The difference between the untreated micromilled samples and the skeletochronology-processed biopsy cores for $\delta^{13}C$ was (mean ± SD) 0·16 ± 0·68‰ (range: −0·86 to 2·33 ‰) and 0·76 ± 0·99‰ for $\delta^{15}N$ (range: −1·94 to 3·40 ‰; Table 2). The $\delta^{13}C$ values were not significantly affected by the skeletochronology treatment based on results from the linear mixed-effects model ($F_{1,58} = 3·14$, $P = 0·08$). There was a slight effect of species on $\delta^{13}C$ values ($F_{1,8} = 5·39$, $P = 0·049$), but there was no interaction between species and skeletochronology treatment ($F_{1,58} = 0·22$, $P = 0·64$; Fig. 3, Table 3). The linear mixed-effects model showed a significant effect of skeletochronology treatment on $\delta^{15}N$ ($F_{1,58} = 38·08$, $P < 0·0001$). Species had no significant effect on $\delta^{15}N$ values ($F_{1,8} = 0·03$, $P = 0·88$), yet there was an interaction between species and skeletochronology treatment ($F_{1,58} = 6·48$, $P = 0·01$; Fig. 3, Tables 2 and 3).

Discussion

COMPARISON OF TWO SEQUENTIAL SAMPLING METHODS

Sequential stable isotope sampling of bone growth layers can provide valuable information regarding animal diet and location over time. We showed that sequential samples from marine turtle bone could effectively be extracted from individual annual growth layers for SIA, thus creating a time series of stable isotope data for individual turtles. The ecological implications of the SIA results from some of the samples used in this study will be the focus of a larger, future study. Here, we presented two methods for sequential sampling of marine turtle bone growth layers, micromilling and biopsy coring, and determined micromilling to be the superior method.

The selection of micromilling as the best sequential sampling method was due to advantages in processing time and costs, ability to precisely sample thin annual layers, and consistency of stable isotope values. Although the cost of the biopsy core punches is low, this method still requires the same microscope equipped with a camera and computer used for the micromilling method. In addition, while the start-up cost of the micromilling software and drill is significant, the per-sample cost is reasonable given the durability and multiple applications of the equipment (e.g. sampling bones, teeth, otoliths and carapace scutes). Finally, while biopsy coring is a quicker process, the micromilling is automated once the sampling path has been programmed. Therefore, the amount of hands-on time required per micromilled sample is comparable to biopsy coring.

In addition, thin annual layers (~0·10–0·25 mm width) can be sampled via micromilling, whereas fine sampling is often impossible with the biopsy coring method, even when a scalpel is used. The diameter of the biopsy tool itself (0·5 mm) limits the annual layers that can be sampled by the biopsy coring method. Further, micromill sampling of individual annual layers is more likely to be contained within the target growth layer, thus increasing sampling precision, whereas the larger biopsy core may inadvertently sample neighbouring growth layers. There is also less sample handling required for micromilling compared to biopsy coring, thus minimizing chances for contamination that could result from repeatedly handling samples.

Table 2. Effect of skeletochronology processing on stable isotope values

Table 2. (continued)

Bone ID	Annual growth layer year	Species	Untreated vs. Skeletochronology processed ($n = 60$)	
			Effect on δ^{13}C (‰)	Effect on δ^{15}N (‰)
A	2007	Cm	0·05	0·30
	2008	Cm	0·26	0·62
	2009	Cm	0·25	0·50
	2010	Cm	0·60	0·77
	2011	Cm	0·16	0·56
B	2006	Cm	−0·26	0·17
	2007	Cm	−0·32	1·05
	2008	Cm	−0·34	−1·94
	2009	Cm	−0·20	−0·12
	2010	Cm	1·28	1·21
	2011	Cm	2·33	3·28
C	1996	Cm	0·37	0·33
	1997	Cm	−0·06	0·67
	1999	Cm	−0·36	1·02
	2002	Cm	0·06	2·37
D	2004	Cm	−0·24	−0·40
	2005	Cm	−0·13	−0·19
	2006	Cm	−0·05	−0·17
	2007	Cm	0·18	1·01
	2008	Cm	0·73	0·54
	2009	Cm	0·12	0·04
E	2005	Cm	0·02	−1·46
	2006	Cm	−0·59	−0·26
	2007	Cm	−0·49	−0·01
	2008	Cm	−0·38	0·22
	2009	Cm	−0·02	0·62
	2010	Cm	0·03	0·40
F	2002	Cc	−0·54	0·75
	2004	Cc	0·26	1·35
	2005	Cc	1·24	2·49
	2006	Cc	1·02	1·80
	2007	Cc	0·90	2·01
	2008	Cc	0·43	1·82
	2009	Cc	1·05	2·71
G	2002	Cc	−0·19	0·06
	2003	Cc	−0·03	0·37
	2004	Cc	−0·86	0·58
	2005	Cc	−0·53	0·34
	2006	Cc	−0·77	−0·08
	2007	Cc	−0·22	0·32
	2008	Cc	−0·10	0·66
H	2001	Cc	−0·50	0·60
	2002	Cc	−0·46	1·37
	2003	Cc	−0·30	0·40
	2004	Cc	−0·59	0·51
	2005	Cc	−0·33	0·70
	2006	Cc	0·06	0·72
	2007	Cc	0·55	1·73
I	2005	Cc	0·00	0·05
	2006	Cc	−0·11	0·18
	2007	Cc	0·58	0·75
	2008	Cc	1·90	2·83
	2009	Cc	1·25	1·95
J	2001	Cc	0·69	0·94
	2003	Cc	−0·20	0·19
	2004	Cc	−0·56	0·12
	2005	Cc	−0·16	0·39
	2006	Cc	−0·08	0·77
	2007	Cc	1·13	1·47
	2008	Cc	1·91	3·40
	AVERAGE:		0·16	0·76
	SD:		0·68	0·99
	$N=$		60	60

Results of the difference between skeletochronology-processed samples and untreated samples for both δ^{13}C and δ^{15}N (δ^{15}N$_{\text{skeletochronology processed bone}}$ − δ^{15}N$_{\text{untreated bone}}$, and similar for δ^{13}C), in permil (‰) units, from individual year growth layers. Values near 0·0 indicate similarity. Sample size represents number of sample pairs. See text for additional details.

Finally, the stable isotope values from the bone powder that was micromilled from the turtle growth layers were more predictable and consistent, and the mechanism driving any effects was understood (Turner Tomaszewicz *et al.* 2015). Samples that had been obtained via biopsy cores, however, were affected, likely by the skeletochronology processing, and the mechanism(s) causing these effects were unclear.

STABLE ISOTOPE ANALYSIS

The δ^{13}C values from the skeletochronology-processed biopsy samples were not affected by the skeletochronology processing to a degree that surpassed the range of stable isotope measurement precision (mean difference was +0·16 ± 0·68 ‰; maximum measurement precision for δ^{13}C was 0·20‰). Yet the maximum difference observed between these groups on δ^{13}C values was >3‰, which is greater than the variation observed for δ^{13}C values from a recent study on the effects of acidification of bone cortical powder for stable isotope analysis (Turner Tomaszewicz *et al.* 2015). Further, the effect of skeletochronology processing on the δ^{13}C values was not consistent or predictable among samples or δ^{13}C values, thereby precluding the development of a useful correction value or equation. Also, the thorough water rinse was assumed to be sufficient for the removal of the storage solvent, glycerine, and a recent study on fish otoliths found no effect of storage in glycerine on δ^{13}C (Gao *et al.* 2015), but the effect of storing bone samples in glycerine was not explicitly tested here. Finally, the mechanism(s) for the observed effects of skeletochronology processing, including glycerine storage, on the δ^{13}C values from bone cores are unknown.

The δ^{15}N values from the skeletochronology-processed biopsy core samples were affected (mean difference was +0·76 ± 0·99‰; maximum measurement precision for δ^{15}N was 0·24‰). We surmise that the effect of skeletochronology processing on the δ^{15}N values was likely related to an unknown
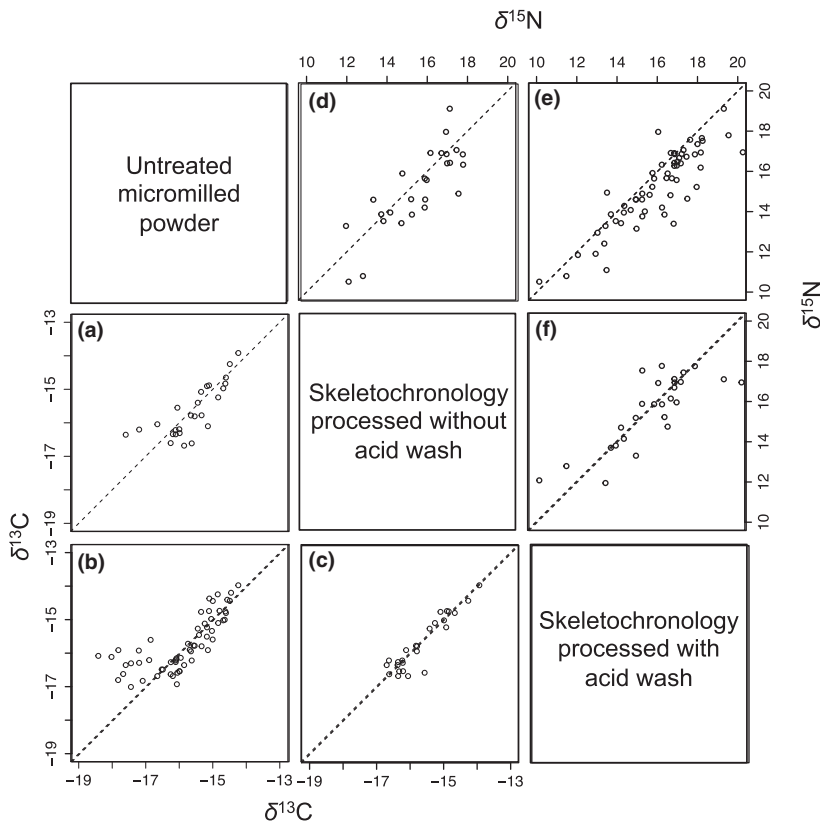
Fig. 3. Effect on SIA of annual biopsy core samples from skeletochronology processing and additional acid wash. Dashed diagonal line shows 1:1 line and represents 'no effect of treatment'. Stable carbon isotope values (δ^{13}C): (a) effect of skeletochronology processing, (b) effect of skeletochronology + acid wash, (c) effect of acid wash on skeletochronology-processed samples. Stable nitrogen isotope values (δ^{15}N): (d) effect of skeletochronology processing, (e) effect of skeletochronology + acid wash, (f) effect of acid wash on skeletochronology-processed samples.

Table 3. Linear mixed-effects models results

	Value	SE	d.f.	*F*-value	*P*-value
Carbon					
(Intercept)	−16·3	0·28	58	6255·19	<0·0001
Species	0·97	0·41	8	5·39	0·049
Skeletochronology Treatment	0·19	0·12	58	3·14	0·08
Species: Skeletochronology Treatment	−0·08	0·18	58	0·22	0·64
Nitrogen					
(Intercept)	14·92	0·67	58	1058·61	<0·0001
Species	0·47	0·96	8	0·03	0·88
Skeletochronology Treatment	1·04	0·17	58	38·08	<0·0001
Species: Skeletochronology Treatment	−0·63	0·25	58	6·48	0·01

Results from linear mixed-effects models. Test effect of species and skeletochronology processing, including acid wash, on biopsy cores. Model: lme(δ^{13}C~ Species*Treatment, random = ~1|Bone_ID/Year). Similar model applied for δ^{15}N.

alteration of the bone's protein-bound nitrogen that occurs during the chemical processing required for skeletochronology. The mechanism(s) causing this alteration of δ^{15}N values remain unknown. Other studies, including Turner Tomaszewicz *et al.* (2015), show that acidification should not affect the δ^{15}N values of cortical bone powder samples. As a result of these potential effects of skeletochronology processing on both the δ^{13}C and δ^{15}N values, we do not recommended using these

types of samples for future SIA when access to unprocessed bone is available.

APPLICATION OF SEQUENTIAL ANNUAL BONE GROWTH LAYERS SAMPLING AND SKELETOCHRONOLOGY

Sequential SIA of growth layers has been conducted on tissues such as otolith and teeth (e.g. Schwarcz *et al.* 1998; Hobson 1999; Newsome *et al.* 2006; McMahon *et al.* 2011; Elorriaga-Verplancken *et al.* 2013) with promising results for migratory megafauna. Only recently has sequential analysis of bone growth layers identified by skeletochronology been attempted (Snover *et al.* 2010; Avens *et al.* 2013), and until now, standard methods for sequential sampling for SIA of δ^{13}C and δ^{15}N values from annual bone layers have not previously been described. The standard protocol presented in the current study, together with the methods for SIA processing of bone in Turner Tomaszewicz *et al.* (2015), allows for the reliable use of δ^{13}C and δ^{15}N values from sequential bone growth layers.

In addition, sequential sampling and SIA of annual growth layers of marine turtle humerus bones provides a continuous, multiyear record of turtle habitat use that cannot be readily collected using traditional techniques. Satellite tag retention for marine turtles is typically on the scale of months to a year, and mark–recapture intervals are rarely annual. These methods gather data from a small fraction of the turtle's life, while the sequential stable isotope sampling presented in this study collects information for multiple, sequential years of a turtle's life, providing new and useful long-term information for marine turtle ecology and conservation.

Recommendations

For researchers utilizing bone growth layers to investigate past diet and location of animals, micromilling of raw, unprocessed, cortical bone powder produces the best samples for stable isotope analysis. The use of chemically processed and biopsy-sampled bone cross sections is not recommended due to affected stable isotope values and the less accurate manual sample extraction procedure. Computer-guided micromilling provided the most accurate and precise sequential sampling method for stable isotope analysis of annual bone growth layers. The stable nitrogen isotope value of untreated whole bone reflects the $\delta^{15}N$ value of the dietary protein consumed at the time of bone synthesis, whereas the $\delta^{13}C$ value of untreated whole bone is slightly higher than the dietary protein alone due to the presence of small amounts of ^{13}C-enriched bioapatite-bound carbonate. Bioapatite can be removed from bone via treatment with acid, and, in a separate paper (Turner Tomaszewicz *et al.* 2015), we present results detailing offset correction values, as well as linear regression equations, to mathematically correct for the $\delta^{13}C$ values from untreated vs. acidified bone powder samples from sea turtles. Sample-specific C:N ratios can be used to ensure that lipid extraction is not necessary (Post *et al.* 2007; Turner Tomaszewicz *et al.* 2015). Ours is the first study to present a standardized method to sequentially sample annual bone growth layers for stable isotope analysis. While tested using bones of marine turtles, these techniques can be applied to a wide variety of both marine and terrestrial vertebrates, and the use of the standard protocol presented here facilitates direct comparison with future studies.

Acknowledgements

Data accessibility

All data used in this publication are provided within the text and in the affiliated Supporting information.

References

Ambrose, S.H. (1990) Preparation and characterization of bone and tooth collagen for isotope analysis. *Journal of Archaeological Science*, **17**, 431–451.

Avens, L., Goshe, L.R., Harms, C.A., Anderson, E.T., Goodman Hall, A., Cluse, W.M. *et al.* (2012) Population characteristics, age structure, and growth dynamics of neritic juvenile green turtles in the northeastern Gulf of Mexico. *Marine Ecology Progress Series*, **458**, 213–229.

Avens, L., Goshe, L.R., Pajuelo, M., Bjorndal, K.A., Macdonald, B.D., Lemons, G.E., Bolten, A.B. & Seminoff, J.A. (2013) Complementary skeletochronology and stable isotope analyses offer new insight into juvenile loggerhead sea turtle oceanic stage duration and growth dynamics. *Marine Ecology Progress Series*, **491**, 235–251.

Burt, N.M. & Garvie-Lok, S. (2013) A new method of dentine microsampling of deciduous teeth for stable isotope ratio analysis. *Journal of Archaeological Science*, **40**, 3854–3864.

Clementz, M.T. & Koch, P.L. (2001) Differentiating aquatic mammal habitat and foraging ecology with stable isotopes in tooth enamel. *Oecologia*, **129**, 461–472.

Dalerum, F. & Angerbjörn, A. (2005) Resolving temporal variation in vertebrate diets using naturally occurring stable isotopes. *Oecologia*, **144**, 647–658.

DeNiro, M.J. & Epstein, S. (1978) Influence of diet on the distribution of carbon isotopes in animals. *Geochimica et Cosmochimica Acta*, **42**, 495–506.

Elorriaga-Verplancken, F., Aurioles-Gamboa, D., Newsome, S.D. & Martínez-Díaz, S.F. (2013) $\delta^{15}N$ and $\delta^{13}C$ values in dental collagen as a proxy for age- and sex-related variation in foraging strategies of California sea lions. *Marine Biology*, **160**, 641–652.

Gao, Y., Crowley, S., Conrad, J. & Dettman, D.L. (2015) Effects of organic solvents on stable isotope composition of otolith and biogenic aragonite. *Paleogeography, Paleoclimatology, Paleoecology*, **440**, 487–495.

Goshe, L.R., Avens, L., Bybee, J. & Hohn, A.A. (2009) An evaluation of histological techniques used in skeletochronological age estimation of sea turtles. *Chelonian Conservation and Biology*, **8**, 217–222.

Goshe, L.R., Avens, L., Scharf, F.S. & Southwood, A.L. (2010) Estimation of age at maturation and growth of Atlantic green turtles (Chelonia mydas) using skeletochronology. *Marine Biology*, **157**, 1725–1740.

Graham, B.S., Koch, P.L., Newsome, S.D., Mcmahon, K.W. & Aurioles, D. (2010) Using Isoscapes to Trace the Movements and Foraging Behavior of Top Predators in Oceanic Ecosystems. *Isoscapes: Understanding Movement, Pattern, and Process on Earth Through Isotope Mapping* (eds J.B. West, G.J. Bowen, T.E. Dawson & K.P. Tu), pp. 299–318. Springer, Dordrecht, Netherlands.

Hobson, K.A. (1999) Tracing origins and migration of wildlife using isotopes: a review. *Oecologia*, **120**, 314–326.

Hobson, K.A., Barnett-Johnson, R. & Cerling, T. (2010) Using Isoscapes to Track Animal Migration. *Isoscapes: Understanding Movement, Pattern, and Process on Earth Through Isotope Mapping* (eds J.B. West, G.J. Bowen, T.E. Dawson & K.P. Tu), pp. 273–298. Springer, Dordrecht, Netherlands.

Koch, P.L., Fogel, M.L. & Tuross, N. (1994) Tracing the diets of fossil animals using stable isotopes. *Stable Isotopes in Ecology and Environmental Science* (eds R. Michener & K. Lajtha), pp. 63–92. Blackwell Publishing Ltd, Malden, MA.

Kurle, C.M. (2009) Interpreting temporal variation in omnivore foraging ecology via stable isotope modelling. *Functional Ecology*, **23**, 733–744.

McMahon, K.W., Hamady, L.I.L. & Thorrold, S.R. (2013) Ocean ecogeochemistry: a review. *Oceanography & Marine Biology: An Annual Review*, **51**, 327–374.

McMahon, K.W., Fogel, M.L., Johnson, B.J., Houghton, L.A. & Thorrold, S.R. (2011) A new method to reconstruct fish diet and movement patterns from $\delta^{13}C$ values in otolith amino acids. *Canadian Journal of Fisheries and Aquatic Sciences*, **68**, 1330–1340.

Michener, R. & Lajtha, K. (eds.) (2007) *Stable Isotopes in Ecology and Environmental Science*, 2nd edn. Blackwell Publishing Ltd., Malden, MA.

Newsome, S.D., Clementz, M.T. & Koch, P.L. (2010) Using stable isotope biogeochemistry to study marine mammal ecology. *Marine Mammal Science*, **26**, 509–572.

Newsome, S.D., Koch, P.L., Etnier, M.A. & Aurioles-Gamboa, D. (2006) Using carbon and nitrogen isotope values to investigate maternal strategies in northeast pacific otariids. *Marine Mammal Science*, **22**, 556–572.

Post, D.M., Layman, C.A., Arrington, D.A., Takimoto, G., Quattrochi, J. & Montaña, C.G. (2007) Getting to the fat of the matter: models, methods and assumptions for dealing with lipids in stable isotope analyses. *Oecologia*, **152**, 179–189.

R Core Team (2013) *R: A Language and Environment for Statistical Computing*. R Foundation for Statistical Computing, Vienna, Austria. URL http://www.R-project.org/.

Rau, G.H., Mearns, A.J., Young, D.R., Olson, R.J., Schafer, H.A. & Kaplan, I.R. (1983) Animal 13C/12C correlates with trophic level in pelagic food webs. *Ecology*, **64**, 1314–1318.

Reich, K.J., Bjorndal, K.A. & Martinez del Rio, C. (2008) Effects of growth and tissue type on the kinetics of 13C and 15N incorporation in a rapidly growing ectotherm. *Oecologia*, **155**, 651–663.

Schoeninger, M.J., Moore, K.M., Murray, M.L. & Kingston, J.D. (1989) Detection of bone preservation in archaeological and fossil samples. *Applied Geochemistry*, **4**, 281–292.

Schwarcz, H.P., Gao, Y., Campana, S., Browne, D., Knyf, M. & Brand, U. (1998) Stable carbon isotope variations in otoliths of Atlantic cod (Gadus morhua). *Canadian Journal of Fisheries and Aquatic Sciences*, **55**, 1798–1806.

Seminoff, J.A., Eguchi, T., Carretta, J., Allen, C.D., Prosperi, D., Rangel, R., Gilpatrick, J.W., Forney, K. & Peckham, S.H. (2014) Loggerhead sea turtle abundance at a foraging hotspot in the eastern Pacific Ocean: implications for at-sea conservation. *Endangered Species Research*, **24**, 207–220.

Snover, M.L. & Hohn, A.A. (2004) Validation and interpretation of annual skeletal marks in loggerhead (*Caretta caretta*) and Kemp's ridley (*Lepidochelys kempii*) sea turtles. *Fisheries Bulletin*, **102**, 682–692.

Snover, M.L., Hohn, A.A., Crowder, L.B. & Macko, S.A. (2010) Combining stable isotopes and skeletal growth marks to detect habitat shifts in juvenile loggerhead sea turtles *Caretta caretta*. *Endangered Species Research*, **13**, 25–31.

Snover, M.L., Hohn, A.A., Goshe, L.R. & Balazs, G.H. (2011) Validation of annual skeletal marks in green sea turtles Chelonia mydas using tetracycline labeling. *Aquatic Biology*, **12**, 197–204.

Turner Tomaszewicz, C., Seminoff, J., Ramirez, M.D. & Kurle, C. (2015) Effects of demineralization on the stable isotope analysis of bone samples. *Rapid Communications in Mass Spectrometry*, **29**, 1879–1888.

Van Klinken, G.J. (1999) Bone collagen quality indicators for palaeodietary and radiocarbon measurements. *Journal of Archaeological Science*, **26**, 687–695.

Vander Zanden, M.J. & Rasmussen, J.B. (2001) Variation in δ^{15}N and δ^{13}C trophic fractionation: Implications for aquatic food web studies. *Limnology and Oceanography*, **46**, 2061–2066.

Supporting Information

Additional Supporting Information may be found in the online version of this article.

Appendix S1. Methods

Figure S1. C:N ratios of biopsy cored skeletochronology samples.

Table S1. Biopsy core acidification experiment.